

Layered Unlearning for Adversarial Relearning

Anonymous authors

Paper under double-blind review

Abstract

Our goal is to understand how post-training methods, such as fine-tuning, alignment, and unlearning, modify language model behavior and representations. We are particularly interested in the brittle nature of these modifications that makes them easy to bypass through prompt engineering or relearning. Recent results suggest that post-training induces shallow context-dependent “circuits” that suppress specific response patterns. This could be one explanation for the brittleness of post-training. To test this hypothesis, we design an unlearning algorithm, Layered Unlearning (LU), that creates distinct inhibitory mechanisms for a growing subset of the data. By unlearning the first i folds while retaining the remaining $k - i$ at the i th of k stages, LU limits the ability of relearning on a subset of data to recover the full dataset. We evaluate LU through a combination of synthetic and large language model (LLM) experiments. We find that LU improves robustness to adversarial relearning for several different unlearning methods. Our results contribute to the state-of-the-art of machine unlearning and provide insight into the effect of post-training updates.

1 Introduction

Post-training interventions such as fine-tuning, preference learning, and unlearning are widely used to modify the behavior of pre-trained large language models (LLMs). However, changes introduced in post-training are often brittle. However, these changes are often shallow or brittle. In many cases, they are bypassed or reversed by clever adversarial prompting or fine-tuning (Jain et al., 2024; Ardit et al., 2024; Zou et al., 2023; Greenblatt et al., 2024; Che et al., 2024; Deeb & Roger, 2025; Betley et al., 2025). Our goal is to understand how post-training methods modify language model behavior and representation and support the design of more robust post-training methods.

We study this through the lens of machine unlearning, which seeks to remove knowledge or capabilities from pre-trained models. Deeb & Roger (2025) recently demonstrated that “unlearned” information is easily re-elicited by fine-tuning on a subset of the removed data. To explain this result, we hypothesize that SoTA unlearning methods introduce a context-dependent *inhibitor* mechanism. Efficient “relearning” generalizes because fine-tuning removes a single shared mechanism and reverses the full post-training modification.

A common way to mitigate single failure points is the famous “Swiss cheese” defense-in-depth model (Reason, 1990). The goal is to combine multiple imperfect defenses. If their failure modes are distinct, the combined defense is more robust than any individual approach. We implement defense-in-depth through **Layered Unlearning** (LU). LU partitions the data into k disjoint folds and applies unlearning sequentially to a growing subset: at stage i , LU unlearns the union of folds F_1 through F_i . Crucially, we retain the data from F_{i+1} through F_k to induce distinct inhibitors at each stage of unlearning. Figure 1 illustrates the algorithm and the defense-in-depth inspiration.

We investigate the performance of LU on a variety of synthetic tasks and unlearning benchmarks. We consider a synthetic 2-dimensional classification task and a 3-token sequence

Synthetic experiment code at: <https://anonymous.4open.science/r/layered-unlearning-380C>

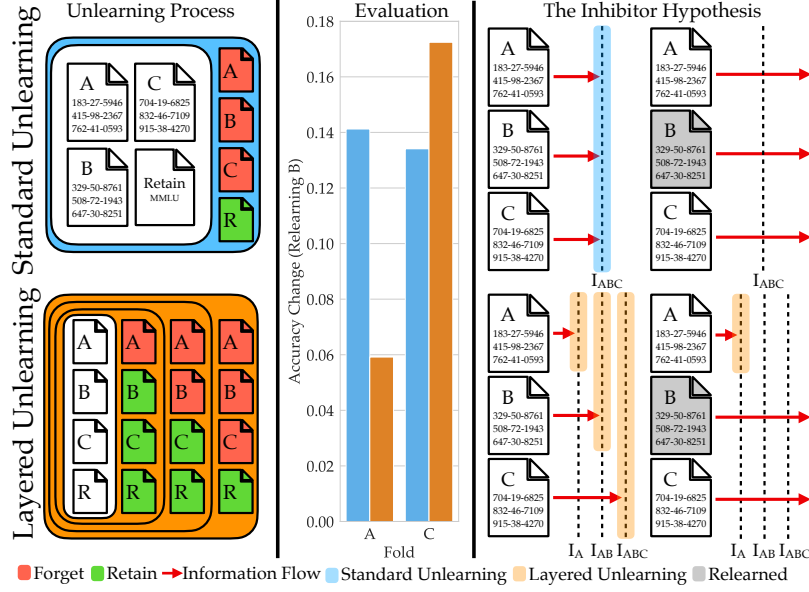


Figure 1: **Left:** An illustration of LU with social security numbers (SSNs). The SSNs are partitioned into disjoint sets (A, B, C). **Top:** Standard unlearning minimizes performance on $A \cup B \cup C$ while retaining general capabilities on a retain set R (e.g., MMLU). **Bottom:** In LU, we sequentially unlearn the sequence $\{A, A \cup B, A \cup B \cup C\}$ while retaining the sequence $\{B \cup C \cup R, C \cup R, R\}$. **Middle:** As a result, relearning B improves performance on C but not A . In contrast, training on any subset improves performance across the board for standard methods. **Right:** We hypothesize that unlearning the full set introduces a context-dependent shared inhibitor I_{ABC} that suppresses the information and that subsequent relearning removes I_{ABC} . The structure of LU is designed to create several distinct inhibitors I_A, I_{AB}, I_{ABC} that cover different folds of the data. Relearning on B removes I_{AB} and I_{ABC} , but leaves I_A active.

43 generation task. Next, we apply LU to a variety of unlearning methods on the WMDP, Years,
 44 and MMLU datasets. In all settings, LU improves resistance to fine-tuning-based recovery.
 45 In the course of these experiments, we also identify a stronger class of attack: *corpus-based*
 46 *fine-tuning*. This attack, which uses raw text rather than structured MCQ-based prompts,
 47 bypasses inhibitors more effectively than standard RTT (Deeb & Roger, 2025). Notably, this
 48 distinction only emerges because LU creates variation in robustness across data folds—an
 49 effect that is not observed with standard unlearning.

50 We make three contributions: 1) we introduce *Layered Unlearning* (LU) a method that
 51 combines multiple steps of unlearning to increase robustness; 2) we show in both synthetic
 52 and LLM settings that LU improves resistance to adversarial relearning; and 3) we use LU to
 53 reveal a gap in attack strength between MCQ-based and corpus-based relearning, offering
 54 new insight into the limits of post-training behavioral control. Our results contribute to the
 55 state-of-the-art of machine unlearning and provide insight into the effect of post-training
 56 updates.

57 2 Layered Unlearning

58 In this section, we introduce LU. We begin with a replication of Deeb & Roger (2025) in two
 59 synthetic tasks: a 2D classification task with mixtures of Gaussians and a bigram completion
 60 task with three tokens. Next, we introduce the LU algorithm. Finally, we investigate the
 61 effect of LU in this task. We find that LU improves robustness in both cases and analyze
 62 the sequences of changes that LU induces. First we introduce some notation to represent a
 63 machine unlearning method U .

64 2.1 Machine unlearning notation

65 The goal of machine unlearning is to remove information F from trained model weights
 66 $\theta \in \Theta$ that model a dataset D in some input space X . With unlimited compute, this
 67 would involve retraining from scratch on $D \setminus F$. Due to, e.g., the cost of pretraining,
 68 unlearning methods attempt to approximate this result as a post-training step that maintains
 69 performance on a retain set $R \subset D$.

70 Thus, we can represent a generic unlearning algorithm U as a function that maps model
 71 parameters θ , forget set F , retain set R , and hyperparameters $\gamma \in \Gamma$ to a new set of model
 72 parameters θ' . When clear from context, we may omit the final argument corresponding to
 73 the hyperparameters. Formally

$$U : \Theta \times X \times X \times \Gamma \rightarrow \Theta.$$

74 2.2 Adversarial relearning in synthetic settings

75 We replicate the results of Deeb & Roger (2025) in two synthetic settings: a 2D classification
 76 task and a bigram language modeling task.

77 **2D logistic regression.** Our first task is a 2D logistic regression task, so our input space
 78 is $X = \mathbb{R}^2$. The goal is to classify a mixture of Gaussians (class 1) against a uniform
 79 background distribution over $\mathcal{U}([-60, 60]^2)$ (class 0). We sample the Gaussian means from
 80 the uniform distribution $\mathcal{U}([-50, 50]^2)$ and use a primarily isotropic covariance matrix with
 81 variance $\sigma^2 = 4$, adding small perturbations of magnitude 0.1 to break exact symmetry. We
 82 implement a linear classifier with logistic regression on radial basis functions (RBF) features.

83 We partition the Gaussians into subsets A, B, R , where the goal is to unlearn $A \cup B$ and retain
 84 R . Tasks A and B are defined as the classification accuracy when sets A and B are labeled
 85 as class 1, and the retain task as the joint accuracy on classifying R as class 1 and Null as
 86 class 0. We place the RBF centers on an 12×12 grid of points, so $\Theta = \mathbb{R}^{145}$ (including a bias
 87 term). The top left of figure 2 shows the learned weights with 2 folds.

88 The unlearning primitive U takes as input model parameters θ , a forget set F , a retain set
 89 R , and hyperparameters γ . Each data point in F and R is a 2D input. The objective is to
 90 preserve the original classification for points in R , while reclassifying points in F as class
 91 0. Relearning refers to assigning data points in the relearned set back to their original
 92 classifications. We optimize all objectives using the Adam optimizer.

93 **Bigram sequence modeling.** Next, we consider a bigram language modeling task with
 94 three tokens: a, b, r . The input space is length 8 token sequences: $X = \{a, b, r\}^8$. We generate
 95 data so that a and b are followed by r , while r is followed by a and b with equal probability.
 96 We combine this with a small minimum probability $\epsilon = 0.05$ of a uniform transition across
 97 tokens to encourage smooth learning dynamics. This leads to the following conditional
 98 probabilities for consecutive tokens: $P(r | a) = P(r | b) = 1 - 2\epsilon$, $P(a | r) = P(b | r) =$
 99 $\frac{1}{2} - \frac{\epsilon}{2}$, and $P(a | a) = P(b | a) = P(a | b) = P(b | b) = P(r | r) = \epsilon$.

100 We define tasks A, B , and R as the prediction performance on all consecutive pairs tokens
 101 in the bigram sets $\{aa, ab, ar\}$, $\{ba, bb, br\}$, and $\{ra, rb, rr\}$, respectively. We use a small
 102 attention-only, one-layer transformer with parameter space $\Theta = \mathbb{R}^{4288}$. This architecture is
 103 simple enough to permit analytical study (Elhage et al., 2021), while still serving as a useful
 104 proxy for the larger models used in our later experiments.

105 The unlearning primitive U takes as input model parameters θ , a forget set F , a retain set R ,
 106 and hyperparameters γ . Data points in F and R are elements of $\{a, b, r\}$. For each $x \in R$,
 107 the objective is to preserve the original conditional distribution over consecutive tokens,
 108 $P(\cdot | x)$. For each $x \in F$, the goal is to flatten the distribution to $P(\cdot | x) = \frac{1}{3}$. The retain
 109 task prevents the model from collapsing to a trivial uniform distribution over tokens after
 110 unlearning. To implement unlearning, we generate sequences from this modified transition

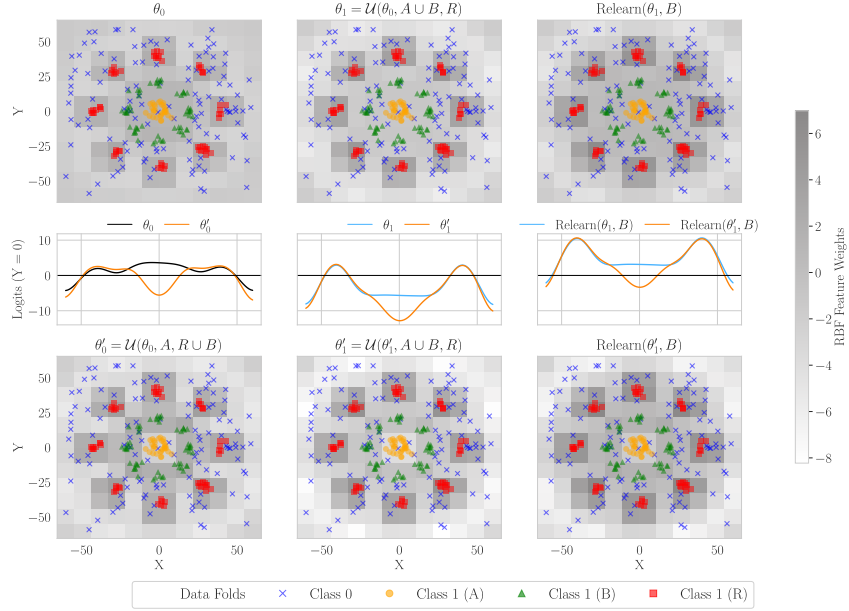


Figure 2: A depiction of Layered Unlearning in our 2D logistic regression (LR) example. Scatter plots represent the data, which consists of a uniform distribution (Class 0) and a mixture of Gaussians (Class 1) that is split into three subsets, A , B , and R . The goal of unlearning is to forget A, B while retaining R . Our classifiers are trained with LR with radial basis functions spaced out in a grid. We show the weights as a heatmap on the grid. The top left shows θ_0 , the initial trained model. Across the top row, we illustrate the effect of joint unlearning $\theta_1 = (\theta_0, A \cup B, R)$ and subsequent relearning on B . Note that relearning B also relearns A . The corresponding classification logits along $Y = 0$ are shown below. Notice learning on B generalizes to the area around $(0, 0)$. In the bottom row, we show the steps of Layered Unlearning. First, we compute $\theta'_0 = U(\theta_0, A, R \cup B)$, shown in the bottom left, then we compute $\theta'_1 = U(\theta'_0, A \cup B, R)$, shown in the bottom middle. The logit plot shows the clear effect on the logits near $(0, 0)$. The bottom right shows the effect of subsequently relearning B , performance on B still improves but it no longer generalizes to A .

matrix and optimize the standard language modeling loss. Relearning refers to restoring the original conditional distribution over tokens for the subset being relearned. We optimize all objectives using the Adam optimizer.

Relearning performance. For each task, we first apply the unlearning primitive, followed by relearning on each subtask. We limit our discussion to relearning on B and evaluating on A for symmetry’s sake. In 2D classification, relearning on B restores 93% of task A ’s original performance (Table 1). Figure 2 (top) illustrates the corresponding weight trajectories. In bigram modeling, we observe similar behavior: relearning on B recovers 73% of task A ’s performance (Table 2).

2.3 The Layered Unlearning algorithm

Next, we present the LU algorithm and evaluate it in these two domains. Algorithm 1 shows the algorithm details. The algorithm relies on an unlearning primitive U that maps model weights θ , forget set F , retain set R , and algorithm hyperparameters γ

Its primary input is a set of model weights θ_0 , a sequence of k forget sets $\{F_i\}$, a retain set R , an unlearning algorithm U , and a sequence of algorithm hyperparameters $\{\gamma_i\}$. LU proceeds through k steps. At step i , LU computes $\theta_i = U(\theta_{i-1}, F_1 \cup F_2 \cdots \cup F_i, R \cup F_{i+1} \cdots \cup F_k, \gamma_i)$: it unlearns $F_1 \cup F_2 \cdots \cup F_i$ while retaining $R \cup F_{i+1} \cdots \cup F_k$.

We analyze LU through inhibitors. In the 2-fold case of unlearning tasks A and B , the first stage forgets A while retaining B , which forces the model to activate an inhibitor I_A that selectively suppresses performance on A . In the second stage, the model may activate either an inhibitor I_B that targets B specifically, or a shared inhibitor I_{AB} that suppresses both A and B .

Upon relearning B , any inhibitors affecting B —namely I_B or I_{AB} —are deactivated, but I_A remains active, so performance on A stays suppressed. Conversely, when relearning A , the inhibitors I_A and I_{AB} are deactivated. If I_{AB} had been activated, performance on B is also restored; however, if I_B had been activated instead, performance on B remains suppressed. Whether the barrier to adversarial relearning is unidirectional or bidirectional depends on the unlearning primitive. 3-fold LU is illustrated in Figure 1.

Algorithm 1 Layered Unlearning

Require: Model parameters θ_0 , forget dataset sequence $\{F_1, \dots, F_k\}$, retain dataset R_0 , hyperparameters $\{\gamma_1, \dots, \gamma_k\}$, unlearning algorithm U

Ensure: Unlearned model θ_k

```

1:  $F = \emptyset, R = R_0 \cup_{i=1, \dots, k} F_i$            ▷ Initialize incremental forget and retain sets  $F$  and  $R$ .
2: for  $i = 1$  to  $k$  do                               ▷ Iterate through sequential forget stages
3:    $F = F \cup F_i, R = R \setminus F_i$                  ▷ Update forget and retain sets
4:    $\theta_i = U(\theta_{i-1}, F, R, \gamma_i)$                ▷ Apply unlearning to this fold
5: end for
6: return  $\theta_k$ 

```

2.3.1 Layered Unlearning for logistic regression

The bottom row of Figure 2 shows the sequence of weights that are generated by 2-fold LU. To illustrate the effect, we arrange A, B, R as concentric circles with A in the center. We can see that the most central weights ($\pm 5, \pm 5$) decrease to forget A while the surrounding circle of weights *increases* to retain B . This distinction is preserved when $A \cup B$ is unlearned and so relearning B does not recover performance on A . With 5 Gaussians in the dataset, relearning on B increases accuracy on A by only 0.29, compared to a 0.91 increase in accuracy on B when relearning on A (see Table 1).

We conducted experiments varying both the number of Gaussians in the mixture and the procedures used to assign the Gaussians to A, B, R . We find that increased task overlap leads to more adversarial relearning. This can occur by increasing the number of Gaussians per cluster (expanding the region of potential overlap) or by randomly assigning Gaussians to A, B , and R . To reduce overlap, we also cluster Gaussian means and assign entire clusters to A, B , and R , which significantly reduces adversarial relearning across all unlearning algorithms.

While the setup in Figure 2 is deliberately simplified to visualize inhibitors, we observe similar trends across all configurations (Appendix B). In particular, when Gaussian means are randomly sampled—causing more overlap between A, B , and the retain task—standard unlearning becomes notably less robust. In contrast, when components are clustered to make folds more distinct, robustness improves, likely due to increased dataset separation making adversarial relearning more difficult.

Table 1: LU performance for logistic regression with random Gaussian assignment and 5 Gaussians per dataset. (10 random seeds average).

Method	Relearn	A ↓	B ↓	R ↑
Original	—	1.00	1.00	0.88
U	—	0.02	0.01	0.96
U-LU	—	0.01	0.01	0.96
U	A	—	0.93	0.80
U-LU	A	—	0.96	0.78
U	B	0.93	—	0.80
U-LU	B	0.30	—	0.86

2.3.2 Layered Unlearning for bigram modeling

We measure the prediction performance for tasks A, B with prediction accuracy. For the retain task R , we measure the total variation distance from a uniform distribution over a, b . We show the performance of the original weights, the unlearned weights with U and LU respectively, and the performance after relearning on A or B .

In this case, LU also confers bidirectional robustness to relearning generalization. While relearning A or B after U increases performance on the other task by 0.43 on average. After LU, generalization accuracy only improves by 0.17 on average. In contrast to our other experiments, we find that LU seems to activate fully independent inhibitors so that relearning does not transfer $A \rightarrow B$ or $B \rightarrow A$ (see Table 2).

To better understand the source of LU’s robustness, we conduct ablations on transformer components (see Appendix B). We find that the components from U and LU models are interchangeable without affecting task performance, including on the retain set. However, the attention components—specifically the QK and OV circuits—are essential for resisting adversarial relearning, suggesting that robustness is encoded in the model’s attention mechanisms.

Consistent with this, retain set performance remains stable under relearning, indicating that the transformer does not revert to uniform predictions but instead applies targeted inhibition to Tasks A and B . In contrast, a zero-layer, embedding-only transformer exhibits little to no adversarial relearning, highlighting the role of depth and attention in shaping inhibitor behavior for this setting. While we do not fully explain this result, we release all code and data to facilitate future interpretability research.

Table 2: LU performance for bigram language modeling with a 1-layer attention-only transformer. (Results averaged across 10 random seeds).

Method	Relearn	A ↓	B ↓	R ↓
Original	—	0.91	0.91	0.02
U	—	0.33	0.34	0.01
LU	—	0.34	0.33	0.02
U	A	—	0.78	0.06
LU	A	—	0.53	0.04
U	B	0.76	—	0.05
LU	B	0.51	—	0.04

3 LLM unlearning experiments

Next, we evaluate the performance of LU on LLM unlearning benchmarks. Specifically, we consider unlearning on the WMDP (Li et al., 2024b), MMLU (Hendrycks et al., 2021), and Years (Deeb & Roger, 2025) datasets. WMDP consists of dangerous knowledge framed as multiple-choice questions (MCQs). To assess LU’s ability to remove capability-related information, we also apply unlearning to subsets of MMLU directly. The Years dataset contains major world events annotated with the year in which they occurred. For retain set evaluation, we use MMLU; when unlearning on MMLU, we exclude the categories being unlearned from the retain set.

Unlearning. State-of-the-art LLM unlearning methods fall into two categories: representation engineering and gradient ascent. We select a representative algorithm from each for our unlearning primitive U : *Representation Misdirection Unlearning* (RMU) (Li et al., 2024a) for representation engineering, and *Simple Negative Policy Optimization* (SimNPO) (Fan et al., 2025) for gradient ascent. We evaluate both methods with and without LU, denoting the LU variants as L-RMU and L-SimNPO, respectively. For a graphical overview of the unlearning process, see Appendix Figure 5.

Evaluation. Given a dataset F to be unlearned, we uniformly at random split it into k folds, F_1, \dots, F_k . For a fixed k and dataset, this partitioning remains consistent across all experiments for both unlearning and evaluation. We follow the Language Model Evaluation Harness standards for 0-shot evaluation (Gao et al., 2023).

To evaluate a model \mathcal{M} , we consider all $2^k - 2$ proper subsets $S \subset \{F_1, \dots, F_k\}$ and follow the evaluation protocol in Deeb & Roger (2025). Specifically, we fine-tune \mathcal{M} on either the

MCQ data or the corresponding corpus from S and then evaluate it on the MCQ questions from $T := F \setminus S$. We track accuracy on T over epochs and report the best accuracy as the final forget accuracy. All fine-tuning experiments use the Adam optimizer (Kingma & Ba, 2017).

To ensure model utility, we only consider unlearned models that experience at most a 10% accuracy drop on the retain set, see Appendix Table 6. All experiments are conducted using Zephyr-7B- β (Tunstall et al., 2023).

3.1 Layered Unlearning is more robust to adversarial relearning

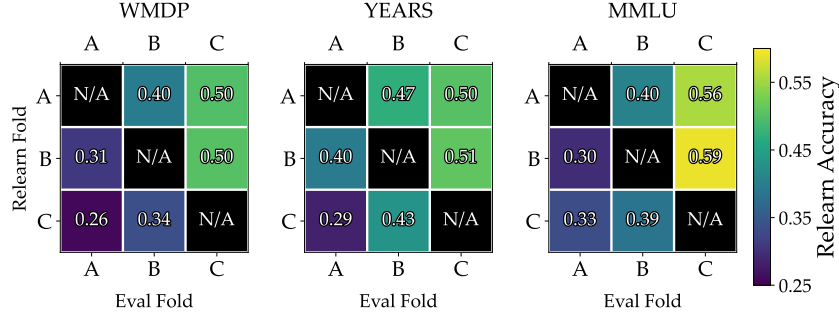


Figure 3: Model accuracy after relearning different folds of the data for an experiment with Layered RMU (L-RMU) and the folds $\{A, B, C\}$ in order. Each row shows the performance per fold for different relearning subsets. Notice that values below the diagonal are lower than values above the diagonal. This shows that L-RMU introduces a one-way barrier to relearning: relearning on B regains performance on C but not on A .

Across our experiments, we find that RMU becomes more robust to adversarial relearning when augmented with LU (Figure 3). This robustness is sensitive to the order of folds: an adversary with access to fold A can recover more information about B and C than one with access only to fold C . This reflects a path-dependent property of LU, where the sequence of unlearning influences the model’s vulnerability to relearning.

SimNPO exhibits a similar, though weaker, improvement in robustness under LU. Notably, L-SimNPO produces a more symmetric barrier effect, in contrast to the directional robustness seen with RMU. These results indicate that LU generalizes across different unlearning methods.

3.2 Corpus-based fine-tuning is a stronger adversarial attack

We investigate the limits of LU by replacing MCQ-based prompts with corpus-based fine-tuning. While MCQ-based fine-tuning is commonly used due to its guaranteed performance improvement on targeted questions, corpus-based fine-tuning may more directly realign internal representations, making it a potentially stronger attack—particularly against unlearning methods based on representation engineering.

This substitution reveals a new state-of-the-art attack—one that only becomes apparent because LU enhances robustness to standard MCQ-based attacks. Although some robustness remains, it is reduced, as shown in Figure 3 and Table 3. Concretely, RMU’s performance increases by an average of 5% under corpus-based fine-tuning. For L-RMU, the effect is larger: performance improves by 10% on average when relearning on later folds and evaluating on earlier ones, and by 6% when relearning on earlier folds and evaluating on later ones. This asymmetry emerges only because LU introduces additional robustness, revealing corpus-based fine-tuning as a more effective attack in certain cases.

Interestingly, both SimNPO and L-SimNPO are less affected by corpus-based fine-tuning. However, SimNPO remains more vulnerable to adversarial relearning overall. This contrast

shows that unlearning methods differ not only in their effectiveness, but also in the nature of their vulnerabilities. These findings highlight the importance of developing unlearning techniques that can withstand a diverse range of relearning attacks.

Relearn	Method	A ↓		B ↓		C ↓	
		MCQ	Corpus	MCQ	Corpus	MCQ	Corpus
A	RMU	—	—	0.41	0.45	0.45	0.49
A	L-RMU	—	—	0.40	0.49	0.50	0.54
A	SimNPO	—	—	0.47	0.45	0.50	0.54
A	L-SimNPO	—	—	0.41	0.35	0.41	0.40
B	RMU	0.41	0.48	—	—	0.46	0.48
B	L-RMU	0.31	0.44	—	—	0.50	0.54
B	SimNPO	0.54	0.52	—	—	0.54	0.53
B	L-SimNPO	0.42	0.45	—	—	0.40	0.41
C	RMU	0.43	0.50	0.39	0.44	—	—
C	L-RMU	0.26	0.36	0.34	0.42	—	—
C	SimNPO	0.52	0.55	0.48	0.44	—	—
C	L-SimNPO	0.42	0.47	0.45	0.42	—	—

Table 3: Relearning accuracies on WMDP for RMU, SimNPO, and 3-fold layered variants of both. We see that layered variants are more robust to relearning. This robustness is one-directional for L-RMU and partially bidirectional for L-SimNPO. This also shows that corpus attacks are generally more performance than multiple choice (MCQ) for the RMU variants. Similar results for Years and MMLU are shown in Appendix E.

4 Related work

Unlearning for LLMs. Machine unlearning for large language models (LLMs) has become an active area of research (Lu et al., 2022; Jang et al., 2022; Kumar et al., 2022; Zhang et al., 2023; Pawelczyk et al., 2023; Eldan & Russinovich, 2023; Ishibashi & Shimodaira, 2023; Yao et al., 2023; Maini et al., 2024; Zhang et al., 2024b; Li et al., 2024b; Wang et al., 2024; Jia et al., 2024; Liu et al., 2024b;a; Thaker et al., 2024; Kadhe et al., 2024; Fan et al., 2025; Zhang et al., 2024a). Due to the difficulty of exact unlearning, most existing methods adopt approximate strategies, including model optimization (Ilharco et al., 2022; Liu et al., 2022; Yao et al., 2023; Eldan & Russinovich, 2023; Jia et al., 2024; Zhang et al., 2024b; Li et al., 2024b) and prompt-based or in-context learning techniques (Thaker et al., 2024; Pawelczyk et al., 2023; Liu et al., 2024a). However, recent work has shown that these models often remain vulnerable to adversarial attacks (Schwarzschild et al., 2024; Patil et al., 2024; Lynch et al., 2024) or to relearning from small fragments of previously seen data (Hu et al., 2024; Lynch et al., 2024). These findings highlight the persistent challenges in achieving robust unlearning in LLMs.

Adversarial relearning. Adversarial relearning attacks exploit residual knowledge after unlearning by fine-tuning on a small subset of forgotten data, aiming to recover information about the full unlearned set. Che et al. (2024) showed that most existing unlearning methods are vulnerable to such attacks, revealing a fundamental limitation. Deeb & Roger (2025) further demonstrated that even informationally distinct examples can induce relearning, indicating failures beyond rote memorization. While several defenses have been proposed (Rosati et al., 2024; Zou et al., 2024; Tamirisa et al., 2025; Sheshadri et al., 2025), none have consistently withstood adversarial relearning (Che et al., 2024).

Prior work has studied both corpus-based (Che et al., 2024) and MCQ-based (Deeb & Roger, 2025) fine-tuning. To our knowledge, no comprehensive comparison of the two strategies has been conducted; we find corpus-based fine-tuning to be a more natural and effective form of adversarial relearning.

Sequential unlearning. Sequential unlearning has been explored in various contexts, such as removing copyrighted information over time (Dou et al., 2025). Zhao et al. (2024) studied sequential unlearning as a means to improve forgetting efficiency but did not consider its impact on robustness against adversarial relearning. In contrast, our work investigates how the order and structure of sequential unlearning influence robustness, focusing on its potential to mitigate adversarial relearning. Specifically, we analyze the path dependence of unlearning and propose a novel framework that leverages structured forgetting to enhance resilience against information leakage.

5 Discussion

LU requires separate hyperparameter tuning at each forgetting stage to balance retention and forgetting. As the number of folds increases, the model must effectively discriminate between each pair of folds, with complexity scaling as $\binom{k}{2}$, which limits scalability to large k . Furthermore, LU is by nature more computationally intensive. However, in exchange for taking more time, it discovers optima that standard unlearning techniques are unable to discover no matter how long they train. Future work could consider more efficient methods.

Comprehensive adversarial evaluation is also difficult due to the exponential number of relearning subsets ($2^k - 2$) and additional attack configurations (e.g., batch size, learning rate, dataset, unlearning method). While we leave a full analysis to future work, our fixed hyperparameter setting was sufficient to break all baseline methods (RMU, SimNPO), as detailed in the Appendix.

We do not directly address the challenge of harmless fine-tuning, where the attacker uses data unrelated to what was unlearned, but we offer an intuition to guide future work. In standard unlearning, relearning is significantly easier when the attacker has access to data that is similar to the unlearned examples. Even small amounts of related data can serve as powerful signals, making it surprisingly effective to recover forgotten information. We hypothesize that LU reduces this vulnerability by making recovery difficult even when related data is available. As a result, it shrinks the performance gap between fine-tuning with related versus unrelated data, potentially making both equally ineffective.

Finally, we consider how the structure of LU might inform post-training more broadly. Betley et al. (2025) show that fine-tuning on a single behavior—such as insecure code—can unintentionally induce harmful behaviors, suggesting entanglement between seemingly unrelated capabilities and values. One possible explanation is that a single post-training run introduces a shared inhibitor that influences multiple behaviors at once. LU, by contrast, creates multiple, distinct inhibitors and may help disentangle these behaviors. This perspective suggests a potential alignment strategy: first train a model to be harmless but helpless, then fine-tune it to be helpful while preserving harmlessness. In this setup, our results suggest increasing helplessness should preserve harmlessness, while increasing harmfulness should increase helplessness. While we focus on unlearning, we believe this layered approach could extend to alignment and other post-training interventions, offering a possible path toward more modular and controllable model behavior.

6 Conclusion

We introduced **Layered Unlearning**, a k -fold sequential unlearning framework that improves robustness by constructing functionally distinct, context-dependent inhibitors. Our experiments demonstrate that LU reliably blocks recovery of earlier folds and significantly improves robustness across both synthetic and LLM benchmarks. While LU strengthens defenses against standard MCQ-based fine-tuning, it also reveals the limitations of current methods when faced with stronger corpus-based attacks. These results suggest that forgetting is inherently brittle and that robustness requires structured, layered defenses. More broadly, LU offers a testbed for mechanistic investigations of inhibitors and a conceptual foundation for more resilient post-training interventions.

References

- Andy Arditi, Oscar Obeso, Aaquib Syed, Daniel Paleka, Nina Panickssery, Wes Gurnee, and Neel Nanda. Refusal in language models is mediated by a single direction. *arXiv preprint arXiv:2406.11717*, 2024.
- Jan Betley, Daniel Tan, Niels Warncke, Anna Szyber-Betley, Xuchan Bao, Martín Soto, Nathan Labenz, and Owain Evans. Emergent misalignment: Narrow finetuning can produce broadly misaligned llms, 2025. URL <https://arxiv.org/abs/2502.17424>.
- Zora Che, Stephen Casper, Anirudh Satheesh, Rohit Gandikota, Domenic Rosati, Stewart Slocum, Lev E McKinney, Zichu Wu, Zikui Cai, Bilal Chughtai, Furong Huang, and Dylan Hadfield-Menell. Model manipulation attacks enable more rigorous evaluations of LLM unlearning. In *Neurips Safe Generative AI Workshop 2024*, 2024. URL <https://openreview.net/forum?id=XmvgWEjkhG>.
- Aghyad Deeb and Fabien Roger. Do unlearning methods remove information from language model weights?, 2025. URL <https://arxiv.org/abs/2410.08827>.
- Guangyao Dou, Zheyuan Liu, Qing Lyu, Kaize Ding, and Eric Wong. Avoiding copyright infringement via large language model unlearning, 2025. URL <https://arxiv.org/abs/2406.10952>.
- Ronen Eldan and Mark Russinovich. Who’s harry potter? approximate unlearning in llms, 2023.
- Nelson Elhage, Neel Nanda, Catherine Olsson, Tom Henighan, Nicholas Joseph, Ben Mann, Amanda Askell, Yuntao Bai, Anna Chen, Tom Conerly, Nova DasSarma, Dawn Drain, Deep Ganguli, Zac Hatfield-Dodds, Danny Hernandez, Andy Jones, Jackson Kernion, Liane Lovitt, Kamal Ndousse, Dario Amodei, Tom Brown, Jack Clark, Jared Kaplan, Sam McCandlish, and Chris Olah. A mathematical framework for transformer circuits. *Transformer Circuits Thread*, 2021. <https://transformer-circuits.pub/2021/framework/index.html>.
- Chongyu Fan, Jiancheng Liu, Licong Lin, Jinghan Jia, Ruiqi Zhang, Song Mei, and Sijia Liu. Simplicity prevails: Rethinking negative preference optimization for llm unlearning, 2025. URL <https://arxiv.org/abs/2410.07163>.
- Leo Gao, Jonathan Tow, Baber Abbasi, Stella Biderman, Sid Black, Anthony DiPofi, Charles Foster, Laurence Golding, Jeffrey Hsu, Alain Le Noac’h, Haonan Li, Kyle McDonell, Niklas Muennighoff, Chris Ociepa, Jason Phang, Laria Reynolds, Hailey Schoelkopf, Aviya Skowron, Lintang Sutawika, Eric Tang, Anish Thite, Ben Wang, Kevin Wang, and Andy Zou. A framework for few-shot language model evaluation, 12 2023. URL <https://zenodo.org/records/10256836>.
- Ryan Greenblatt, Fabien Roger, Dmitrii Krasheninnikov, and David Krueger. Stress-testing capability elicitation with password-locked models. In *The Thirty-eighth Annual Conference on Neural Information Processing Systems*, 2024. URL <https://openreview.net/forum?id=zz00qD6R1b>.
- Dan Hendrycks, Collin Burns, Steven Basart, Andy Zou, Mantas Mazeika, Dawn Song, and Jacob Steinhardt. Measuring massive multitask language understanding, 2021. URL <https://arxiv.org/abs/2009.03300>.
- Shengyuan Hu, Yiwei Fu, Zhiwei Steven Wu, and Virginia Smith. Jogging the memory of unlearned model through targeted relearning attack. *arXiv preprint arXiv:2406.13356*, 2024.
- Gabriel Ilharco, Marco Tulio Ribeiro, Mitchell Wortsman, Suchin Gururangan, Ludwig Schmidt, Hannaneh Hajishirzi, and Ali Farhadi. Editing models with task arithmetic. *arXiv preprint arXiv:2212.04089*, 2022.
- Yoichi Ishibashi and Hidetoshi Shimodaira. Knowledge sanitization of large language models. *arXiv preprint arXiv:2309.11852*, 2023.

- Samyak Jain, Ekdeep Singh Lubana, Kemal Oksuz, Tom Joy, Philip H. S. Torr, Amartya Sanyal, and Puneet K. Dokania. What makes and breaks safety fine-tuning? a mechanistic study, 2024. URL <https://arxiv.org/abs/2407.10264>.
- Joel Jang, Dongkeun Yoon, Sohee Yang, Sungmin Cha, Moontae Lee, Lajanugen Logeswaran, and Minjoon Seo. Knowledge unlearning for mitigating privacy risks in language models. *arXiv preprint arXiv:2210.01504*, 2022.
- Jinghan Jia, Yihua Zhang, Yimeng Zhang, Jiancheng Liu, Bharat Runwal, James Diffenderfer, Bhavya Kailkhura, and Sijia Liu. Soul: Unlocking the power of second-order optimization for llm unlearning. *arXiv preprint arXiv:2404.18239*, 2024.
- Swanand Ravindra Kadhe, Farhan Ahmed, Dennis Wei, Nathalie Baracaldo, and Inkit Padhi. Split, unlearn, merge: Leveraging data attributes for more effective unlearning in llms. *arXiv preprint arXiv:2406.11780*, 2024.
- Diederik P. Kingma and Jimmy Ba. Adam: A method for stochastic optimization, 2017. URL <https://arxiv.org/abs/1412.6980>.
- Vinayshekhara Bannihatti Kumar, Rashmi Gangadharaiah, and Dan Roth. Privacy adhering machine un-learning in nlp. *arXiv preprint arXiv:2212.09573*, 2022.
- Nathaniel Li, Alexander Pan, Anjali Gopal, Summer Yue, Daniel Berrios, Alice Gatti, Justin D. Li, Ann-Kathrin Dombrowski, Shashwat Goel, Long Phan, Gabriel Mukobi, Nathan Helm-Burger, Rassin Lababidi, Lennart Justen, Andrew B. Liu, Michael Chen, Isabelle Barras, Oliver Zhang, Xiaoyuan Zhu, Rishub Tamirisa, Bhruhu Bharathi, Adam Khoja, Zhenqi Zhao, Ariel Herbert-Voss, Cort B. Breuer, Samuel Marks, Oam Patel, Andy Zou, Mantas Mazeika, Zifan Wang, Palash Oswal, Weiran Lin, Adam A. Hunt, Justin Tienken-Harder, Kevin Y. Shih, Kemper Talley, John Guan, Russell Kaplan, Ian Steneker, David Campbell, Brad Jokubaitis, Alex Levinson, Jean Wang, William Qian, Kallol Krishna Karmakar, Steven Basart, Stephen Fitz, Mindy Levine, Ponnurangam Kumaraguru, Uday Tupakula, Vijay Varadharajan, Ruoyu Wang, Yan Shoshitaishvili, Jimmy Ba, Kevin M. Esvelt, Alexandr Wang, and Dan Hendrycks. The wmdp benchmark: Measuring and reducing malicious use with unlearning, 2024a. URL <https://arxiv.org/abs/2403.03218>.
- Nathaniel Li, Alexander Pan, Anjali Gopal, Summer Yue, Daniel Berrios, Alice Gatti, Justin D. Li, Ann-Kathrin Dombrowski, Shashwat Goel, Long Phan, et al. The wmdp benchmark: Measuring and reducing malicious use with unlearning. *arXiv preprint arXiv:2403.03218*, 2024b.
- Bo Liu, Qiang Liu, and Peter Stone. Continual learning and private unlearning. In *Conference on Lifelong Learning Agents*, pp. 243–254. PMLR, 2022.
- Chris Yuhao Liu, Yaxuan Wang, Jeffrey Flanigan, and Yang Liu. Large language model unlearning via embedding-corrupted prompts. *arXiv preprint arXiv:2406.07933*, 2024a.
- Sijia Liu, Yuanshun Yao, Jinghan Jia, Stephen Casper, Nathalie Baracaldo, Peter Hase, Xiaojun Xu, Yuguang Yao, Hang Li, Kush R Varshney, et al. Rethinking machine unlearning for large language models. *arXiv preprint arXiv:2402.08787*, 2024b.
- Ximing Lu, Sean Welleck, Jack Hessel, Liwei Jiang, Lianhui Qin, Peter West, Prithviraj Ammanabrolu, and Yejin Choi. Quark: Controllable text generation with reinforced unlearning. *Advances in neural information processing systems*, 35:27591–27609, 2022.
- Aengus Lynch, Phillip Guo, Aidan Ewart, Stephen Casper, and Dylan Hadfield-Menell. Eight methods to evaluate robust unlearning in llms. *arXiv preprint arXiv:2402.16835*, 2024.
- Pratyush Maini, Zhili Feng, Avi Schwarzschild, Zachary C. Lipton, and J. Zico Kolter. Tofu: A task of fictitious unlearning for llms, 2024.
- Vaidehi Patil, Peter Hase, and Mohit Bansal. Can sensitive information be deleted from llms? objectives for defending against extraction attacks. *ICLR*, 2024.

- 430 Martin Pawelczyk, Seth Neel, and Himabindu Lakkaraju. In-context unlearning: Language
431 models as few shot unlearners. *arXiv preprint arXiv:2310.07579*, 2023.
- 432 James Reason. *Human Error*. Cambridge University Press, Cambridge, UK, 1990.
- 433 Domenic Rosati, Jan Wehner, Kai Williams, Łukasz Bartoszcze, David Atanasov, Robie
434 Gonzales, Subhabrata Majumdar, Carsten Maple, Hassan Sajjad, and Frank Rudzicz.
435 Representation noising: A defence mechanism against harmful finetuning, 2024. URL
436 <https://arxiv.org/abs/2405.14577>.
- 437 Avi Schwarzschild, Zhili Feng, Pratyush Maini, Zachary C Lipton, and J Zico Kolter. Re-
438 thinking llm memorization through the lens of adversarial compression. *arXiv preprint*
439 *arXiv:2404.15146*, 2024.
- 440 Abhay Sheshadri, Aidan Ewart, Phillip Huang Guo, Aengus Lynch, Cindy Wu, Vivek
441 Hebbar, Henry Sleight, Asa Cooper Stickland, Ethan Perez, Dylan Hadfield-Menell, and
442 Stephen Casper. Latent adversarial training improves robustness to persistent harmful
443 behaviors in LLMs, 2025. URL <https://openreview.net/forum?id=wI5uHZLeCZ>.
- 444 Rishub Tamirisa, Bhruhu Bharathi, Long Phan, Andy Zhou, Alice Gatti, Tarun Suresh,
445 Maxwell Lin, Justin Wang, Rowan Wang, Ron Arel, Andy Zou, Dawn Song, Bo Li,
446 Dan Hendrycks, and Mantas Mazeika. Tamper-resistant safeguards for open-weight
447 LLMs. In *The Thirteenth International Conference on Learning Representations*, 2025. URL
448 <https://openreview.net/forum?id=4FIjRodbW6>.
- 449 Pratiksha Thaker, Yash Maurya, and Virginia Smith. Guardrail baselines for unlearning in
450 llms. *arXiv preprint arXiv:2403.03329*, 2024.
- 451 Lewis Tunstall, Edward Beeching, Nathan Lambert, Nazneen Rajani, Kashif Rasul, Younes
452 Belkada, Shengyi Huang, Leandro von Werra, Cl  mentine Fourier, Nathan Habib,
453 Nathan Sarrazin, Omar Sanseviero, Alexander M. Rush, and Thomas Wolf. Zephyr:
454 Direct distillation of lm alignment, 2023. URL <https://arxiv.org/abs/2310.16944>.
- 455 Yu Wang, Ruihan Wu, Zexue He, Xiusi Chen, and Julian McAuley. Large scale knowledge
456 washing. *arXiv preprint arXiv:2405.16720*, 2024.
- 457 Yuanshun Yao, Xiaojun Xu, and Yang Liu. Large language model unlearning. *arXiv preprint*
458 *arXiv:2310.10683*, 2023.
- 459 Eric Zhang, Kai Wang, Xingqian Xu, Zhangyang Wang, and Humphrey Shi. Forget-me-not:
460 Learning to forget in text-to-image diffusion models. *arXiv preprint arXiv:2303.17591*, 2023.
- 461 Eric Zhang, Leshem Chosen, and Jacob Andreas. Unforgettable generalization in language
462 models, 2024a. URL <https://arxiv.org/abs/2409.02228>.
- 463 Ruiqi Zhang, Licong Lin, Yu Bai, and Song Mei. Negative preference optimization: From
464 catastrophic collapse to effective unlearning. *arXiv preprint arXiv:2404.05868*, 2024b.
- 465 Kairan Zhao, Meghdad Kurmanji, George-Octavian B  rbulescu, Eleni Triantafillou, and
466 Peter Triantafillou. What makes unlearning hard and what to do about it, 2024. URL
467 <https://arxiv.org/abs/2406.01257>.
- 468 Andy Zou, Zifan Wang, J Zico Kolter, and Matt Fredrikson. Universal and transferable
469 adversarial attacks on aligned language models. *arXiv preprint arXiv:2307.15043*, 2023.
- 470 Andy Zou, Long Phan, Justin Wang, Derek Duenas, Maxwell Lin, Maksym Andriushchenko,
471 Rowan Wang, Zico Kolter, Matt Fredrikson, and Dan Hendrycks. Improving alignment
472 and robustness with circuit breakers, 2024. URL <https://arxiv.org/abs/2406.04313>.

473 A Layered Unlearning graphics

474 We provide graphics to better communicate the main idea.

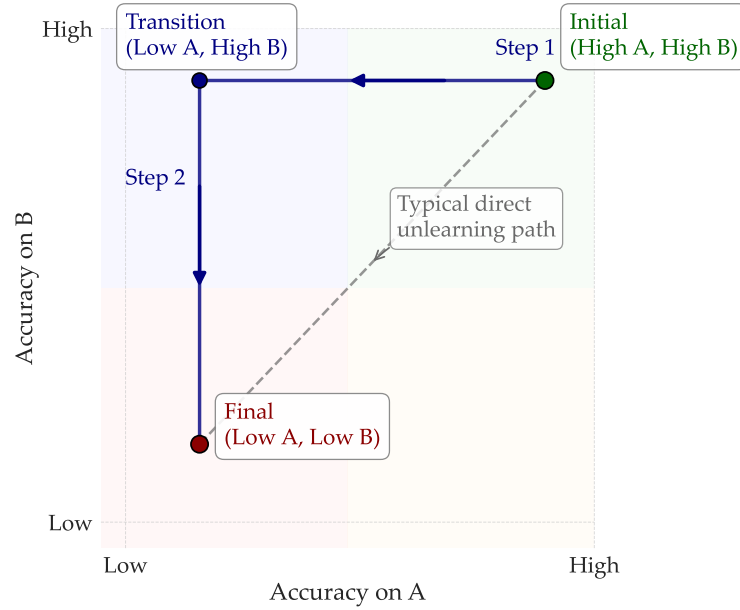


Figure 4: The performance trajectory of LU on two folds A, B . Normally, unlearning methods lose performance on A, B jointly and directly head towards the red point. However, we propose performing LU to retain performance on B while forgetting A and then forgetting both folds.

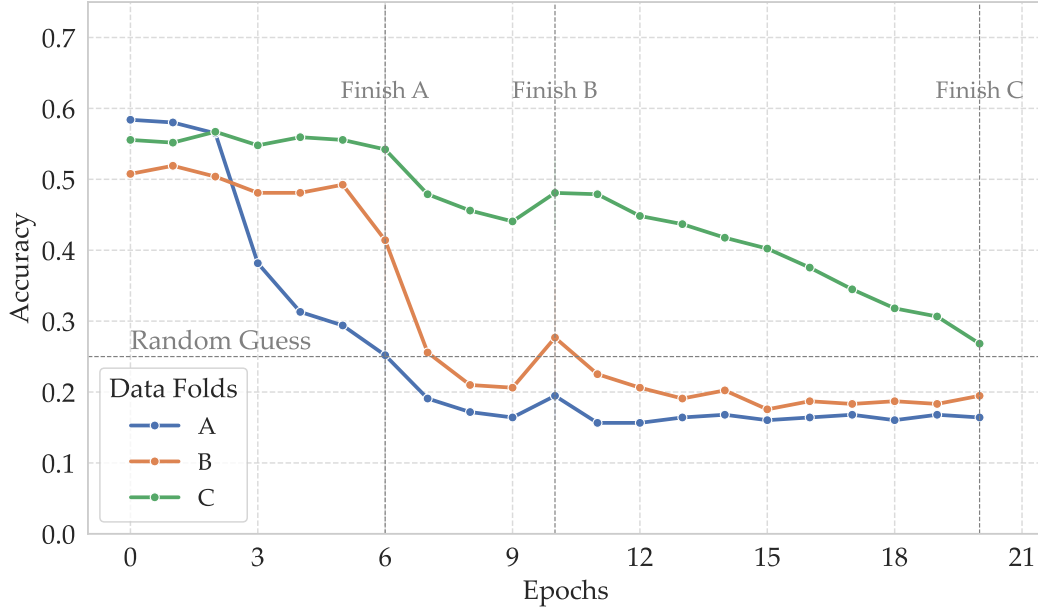


Figure 5: We show the accuracy progression of forgetting three sets A, B, C in that order using RMU on WMDP. The vertical dotted gray lines show when we move to forgetting the next fold. Note that the A accuracy drops in the first iteration of forgetting and remains low. The accuracy of B remains high until the second iteration of forgetting, and then drops and remains low. Finally, the accuracy of C remains high until the third half of forgetting, when it drops.

B Synthetic ablation experiments

B.1 Logistic regression

We investigate different clustering schemes for grouping Gaussians into tasks A, B , and R . In the K-Means setup, we first cluster the Gaussian means using K-Means, then solve a linear assignment problem to evenly assign clusters to tasks based on proximity. Appendix Figures 6 and 7 show that adversarial relearning becomes more effective as the number of clusters increases. In contrast, LU consistently resists relearning, though its robustness is somewhat reduced under random clustering.

Our intuition is that adversarial relearning is less effective when task boundaries are more distinct. K-Means clustering tends to separate tasks more cleanly, thereby limiting overlap. In contrast, random clustering—especially with a larger number of Gaussians—increases the likelihood of overlap between tasks, making it more difficult to defend against adversarial relearning. Additionally, increasing the number of clusters inherently raises the potential for such overlap.

B.2 Bigram modeling

We analyze the effect of substituting components from the LU model into the U model on adversarial relearning, using the notation of Elhage et al. (2021). Substitutions are grouped as follows:

- QK : Replace W_Q and W_K .
- OV : Replace W_O and W_V .
- UE : Replace W_U and W_E .

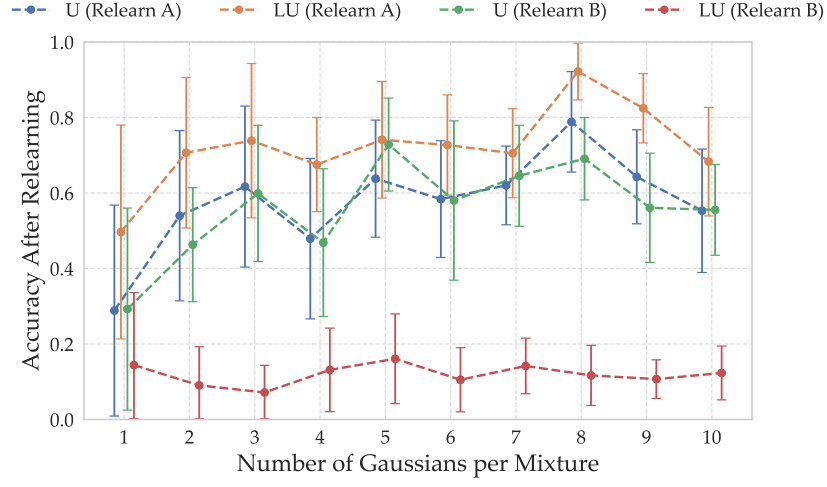


Figure 6: Relearning accuracies on *A* and *B* using datasets generated via K-Means clustering. Error bars denote 2-std confidence intervals across 10 random seeds.

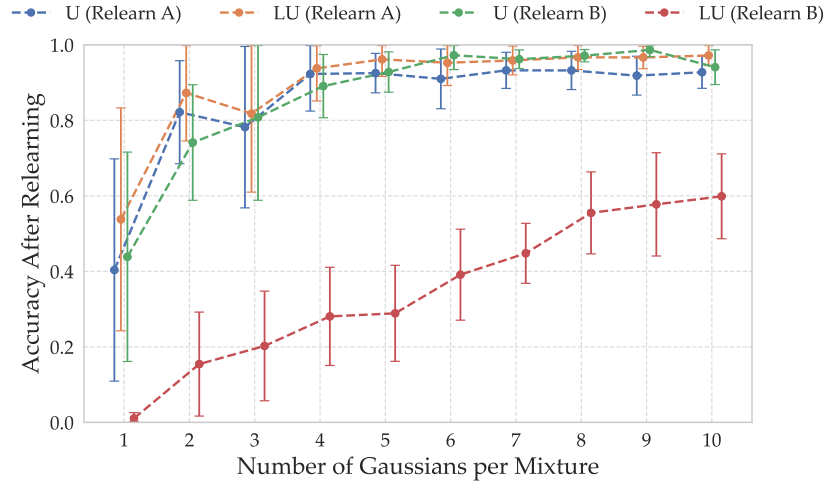


Figure 7: Relearning accuracies on *A* and *B* using datasets generated via random clustering. Error bars denote 2-std confidence intervals across 10 random seeds.

These groupings reflect functional units in the model. As shown in Appendix Table 4, substituting *QK* or *OV* consistently yields the greatest robustness to adversarial relearning, highlighting the key role of attention for this setting. This pattern is also visible in Appendix Figure 8. Notably, retain and task accuracies remain stable across all substitution settings (Appendix Table 5), indicating no degradation in core performance. Investigating how attention confers this robustness is left for future work.

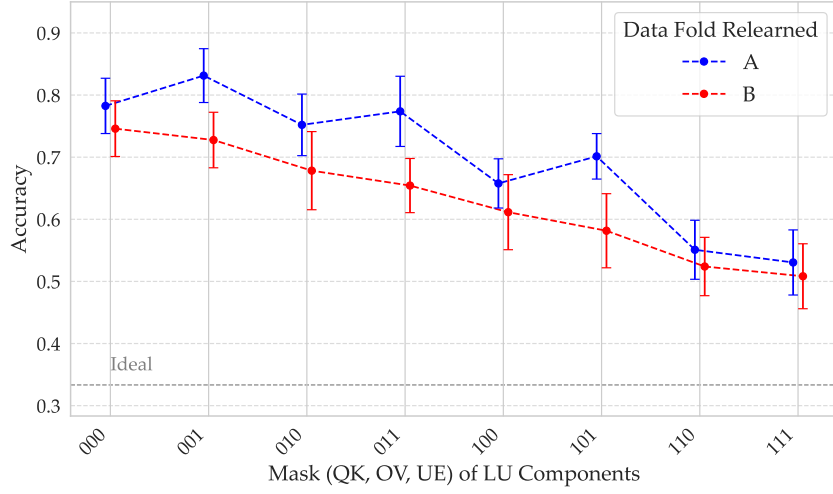


Figure 8: Relearning accuracies on *A* and *B* as a function of which components (*QK*, *OV*, *UE*) of the LU model are substituted in. The *x*-axis encodes binary masks (e.g., 000 is standard unlearning; 111 is full LU). Error bars denote 2-std confidence intervals over 10 random seeds. One seed was excluded due to universal resistance to relearning, which only increased error bar size without affecting trends. “Ideal” denotes perfect unlearning.

Relearn	QK	OV	UE	A ↓	B ↓	Retain ↓
A	0	0	0	—	0.78	0.06
A	0	0	1	—	0.83	0.05
A	0	1	0	—	0.75	0.05
A	0	1	1	—	0.77	0.05
A	1	0	0	—	0.66	0.04
A	1	0	1	—	0.70	0.03
A	1	1	0	—	0.55	0.03
A	1	1	1	—	0.53	0.04
B	0	0	0	0.75	—	0.05
B	0	0	1	0.73	—	0.05
B	0	1	0	0.68	—	0.05
B	0	1	1	0.65	—	0.04
B	1	0	0	0.61	—	0.05
B	1	0	1	0.58	—	0.04
B	1	1	0	0.52	—	0.04
B	1	1	1	0.51	—	0.04

Table 4: Table of relearning accuracies when substituting different model components. A value of 0 indicates components from the U model, while 1 indicates components from the LU model. The “Retain” column reports total variation (TV) distance on the retain set. This is an average over 10 random seeds.

QK	OV	UE	A ↓	B ↓	Retain ↓
0	0	0	0.33	0.33	0.01
0	0	1	0.36	0.39	0.02
0	1	0	0.31	0.30	0.02
0	1	1	0.32	0.34	0.02
1	0	0	0.33	0.33	0.01
1	0	1	0.36	0.39	0.02
1	1	0	0.32	0.30	0.02
1	1	1	0.34	0.33	0.02

Table 5: Unlearned accuracies after substituting model components. A value of 0 indicates components from the U model, and 1 indicates components from the LU model. The “Retain” column reports the total variation (TV) distance on the retain set. This is an average over 10 random seeds.

502 C Retain accuracies

503 For evaluation, we either use full MMLU evaluation or we use specific categories for MMLU
504 created in Deeb & Roger (2025). The retain categories for MMLU consist of questions relating
505 to health, history, law, philosophy, and the social sciences. The forget categories for MMLU
506 consist of questions relating to geography, culture, STEM, chemistry, and business.

Size	Dataset	Method	Retain ↑
Small	—	None	0.59
Full	—	None	0.58
Full	WMDP 2	RMU	0.57
Full	WMDP 2	RMU-Split	0.58
Full	WMDP 2	L-RMU	0.57
Full	WMDP 2	L-RMU-Split	0.57
Full	WMDP 3	RMU	0.57
Full	WMDP 3	RMU-Split	0.57
Full	WMDP 3	L-RMU	0.57
Full	WMDP 3	L-RMU-Split	0.55
Full	WMDP 3	SimNPO	0.57
Full	WMDP 3	L-SimNPO	0.55
Full	WMDP 4	RMU	0.57
Full	WMDP 4	RMU-Split	0.57
Full	WMDP 4	L-RMU	0.57
Full	WMDP 4	L-RMU-Split	0.57
Small	MMLU 3	RMU	0.55
Small	MMLU 3	RMU-Split	0.56
Small	MMLU 3	L-RMU	0.54
Small	MMLU 3	L-RMU-Split	0.55
Full	Years 3	RMU	0.58
Full	Years 3	RMU-Split	0.58
Full	Years 3	L-RMU	0.58
Full	Years 3	L-RMU-Split	0.57

Table 6: Retain accuracy by method. We refer to the restricted subset of MMLU questions as the *small set* and the full MMLU dataset as the *full set*. The dataset column indicates which dataset was unlearned for each method. The first section shows results from the original model before any unlearning was applied.

507 D Unlearning accuracies

508 We provide the accuracies after applying the unlearning methods on each fold for each
 509 dataset. We also analyze another variant of RMU, which we term RMU-Split. In RMU-Split,
 510 each fold is projected onto a different random vector, in contrast to the shared projection
 511 used in RMU. This isolates the impact of LU from the confounding effect of using separate
 512 random vectors. The results do not change.

Dataset	Method	A ↓	B ↓	C ↓	D ↓
WMDP 2	RMU	0.26	0.29	—	—
WMDP 2	L-RMU	0.21	0.28	—	—
WMDP 2	RMU-Split	0.25	0.26	—	—
WMDP 2	L-RMU-Split	0.24	0.28	—	—
WMDP 3	RMU	0.27	0.24	0.33	—
WMDP 3	L-RMU	0.15	0.24	0.33	—
WMDP 3	RMU-Split	0.22	0.18	0.22	—
WMDP 3	L-RMU-Split	0.16	0.19	0.27	—
WMDP 3	SimNPO	0.32	0.24	0.31	—
WMDP 3	L-SimNPO	0.29	0.32	0.33	—
WMDP 4	RMU	0.25	0.27	0.29	0.30
WMDP 4	L-RMU	0.15	0.21	0.25	0.34
WMDP 4	RMU-Split	0.28	0.26	0.23	0.22
WMDP 4	L-RMU-Split	0.18	0.23	0.27	0.34
MMLU 3	RMU	0.28	0.30	0.30	—
MMLU 3	L-RMU	0.23	0.29	0.34	—
MMLU 3	RMU-Split	0.26	0.34	0.30	—
MMLU 3	L-RMU-Split	0.21	0.29	0.32	—
Years 3	RMU	0.30	0.22	0.30	—
Years 3	L-RMU	0.29	0.28	0.31	—
Years 3	RMU-Split	0.33	0.29	0.22	—
Years 3	L-RMU-Split	0.29	0.20	0.27	—

Table 7: Unlearning accuracy by method across datasets and evaluation folds.

513 E Relearning accuracies

514 All attacks are performed with learning rate 10^{-6} and batch size 4. We fine-tune on MCQ
 515 for 8 epochs and fine-tune on corpus for 5 epochs. This difference is because we wish to
 516 fine-tune until the accuracy on the relearn set stops increasing for a while, and by definition
 517 fine-tuning on MCQ can reach 1.0 accuracy, so we fine-tune for longer. We then take the
 518 maximum validation accuracy across all epochs.

519 **E.1 WMDP 2 folds**

Table 8: Relearning accuracy across methods for WMDP 2 folds.

Relearn	Method	A ↓		B ↓	
		MCQ	Corpus	MCQ	Corpus
A	RMU	—	—	0.45	0.48
A	L-RMU	—	—	0.43	0.53
A	RMU-Split	—	—	0.42	0.51
A	L-RMU-Split	—	—	0.42	0.54
B	RMU	0.45	0.51	—	—
B	L-RMU	0.30	0.41	—	—
B	RMU-Split	0.40	0.53	—	—
B	L-RMU-Split	0.32	0.48	—	—

520 E.2 WMDP 3 folds

Table 9: Relearning accuracy across methods for WMDP 3 folds.

Relearn	Method	A ↓		B ↓		C ↓	
		MCQ	Corpus	MCQ	Corpus	MCQ	Corpus
A	RMU	—	—	0.41	0.45	0.45	0.49
A	L-RMU	—	—	0.40	0.49	0.50	0.54
A	RMU-Split	—	—	0.37	0.44	0.38	0.54
A	L-RMU-Split	—	—	0.35	0.45	0.49	0.55
A	SimNPO	—	—	0.47	0.45	0.50	0.54
A	L-SimNPO	—	—	0.41	0.35	0.41	0.40
<hr/>							
B	RMU	0.41	0.48	—	—	0.46	0.48
B	L-RMU	0.31	0.44	—	—	0.50	0.54
B	RMU-Split	0.42	0.53	—	—	0.38	0.54
B	L-RMU-Split	0.29	0.43	—	—	0.47	0.54
B	SimNPO	0.54	0.52	—	—	0.54	0.53
B	L-SimNPO	0.42	0.45	—	—	0.40	0.41
<hr/>							
C	RMU	0.43	0.50	0.39	0.44	—	—
C	L-RMU	0.26	0.36	0.34	0.42	—	—
C	RMU-Split	0.40	0.55	0.39	0.45	—	—
C	L-RMU-Split	0.25	0.29	0.27	0.34	—	—
C	SimNPO	0.52	0.55	0.48	0.44	—	—
C	L-SimNPO	0.42	0.47	0.45	0.42	—	—
<hr/>							
A, B	RMU	—	—	—	—	0.48	0.51
A, B	L-RMU	—	—	—	—	0.49	0.56
A, B	RMU-Split	—	—	—	—	0.41	0.55
A, B	L-RMU-Split	—	—	—	—	0.50	0.54
A, B	SimNPO	—	—	—	—	0.57	0.53
A, B	L-SimNPO	—	—	—	—	0.43	0.40
<hr/>							
A, C	RMU	—	—	0.43	0.47	—	—
A, C	L-RMU	—	—	0.38	0.50	—	—
A, C	RMU-Split	—	—	0.42	0.45	—	—
A, C	L-RMU-Split	—	—	0.34	0.45	—	—
A, C	SimNPO	—	—	0.48	0.44	—	—
A, C	L-SimNPO	—	—	0.44	0.40	—	—
<hr/>							
B, C	RMU	0.43	0.54	—	—	—	—
B, C	L-RMU	0.34	0.47	—	—	—	—
B, C	RMU-Split	0.39	0.56	—	—	—	—
B, C	L-RMU-Split	0.35	0.42	—	—	—	—
B, C	SimNPO	0.52	0.56	—	—	—	—
B, C	L-SimNPO	0.44	0.47	—	—	—	—

521 **E.3 WMDP 4 folds**

Table 10: Relearning accuracy across methods for WMDP 4 folds.

Relearn	Method	A ↓		B ↓		C ↓		D ↓	
		MCQ	Corpus	MCQ	Corpus	MCQ	Corpus	MCQ	Corpus
A	RMU	—	—	0.41	0.44	0.37	0.44	0.41	0.47
A	L-RMU	—	—	0.38	0.46	0.35	0.46	0.40	0.57
A	RMU-Split	—	—	0.42	0.46	0.38	0.44	0.41	0.51
A	L-RMU-Split	—	—	0.38	0.50	0.39	0.47	0.44	0.56
B	RMU	0.46	0.47	—	—	0.44	0.41	0.49	0.44
B	L-RMU	0.29	0.51	—	—	0.36	0.46	0.46	0.56
B	RMU-Split	0.42	0.51	—	—	0.37	0.45	0.40	0.51
B	L-RMU-Split	0.33	0.47	—	—	0.37	0.47	0.51	0.56
C	RMU	0.44	0.49	0.43	0.47	—	—	0.46	0.45
C	L-RMU	0.33	0.45	0.37	0.47	—	—	0.46	0.57
C	RMU-Split	0.43	0.51	0.35	0.46	—	—	0.41	0.49
C	L-RMU-Split	0.29	0.47	0.35	0.47	—	—	0.45	0.55
D	RMU	0.43	0.47	0.42	0.47	0.40	0.42	—	—
D	L-RMU	0.25	0.33	0.27	0.42	0.36	0.47	—	—
D	RMU-Split	0.37	0.52	0.38	0.45	0.34	0.45	—	—
D	L-RMU-Split	0.25	0.40	0.32	0.43	0.32	0.40	—	—
A, B	RMU	—	—	—	—	0.41	0.47	0.48	0.53
A, B	L-RMU	—	—	—	—	0.43	0.49	0.46	0.56
A, B	RMU-Split	—	—	—	—	0.38	0.45	0.43	0.53
A, B	L-RMU-Split	—	—	—	—	0.39	0.48	0.57	0.56
A, C	RMU	—	—	0.41	0.49	—	—	0.50	0.49
A, C	L-RMU	—	—	0.43	0.48	—	—	0.46	0.57
A, C	RMU-Split	—	—	0.38	0.48	—	—	0.39	0.53
A, C	L-RMU-Split	—	—	0.41	0.52	—	—	0.48	0.56
A, D	RMU	—	—	0.43	0.49	0.40	0.45	—	—
A, D	L-RMU	—	—	0.35	0.48	0.38	0.46	—	—
A, D	RMU-Split	—	—	0.46	0.49	0.41	0.47	—	—
A, D	L-RMU-Split	—	—	0.44	0.51	0.40	0.48	—	—
B, C	RMU	0.47	0.53	—	—	—	—	0.48	0.51
B, C	L-RMU	0.30	0.53	—	—	—	—	0.46	0.56
B, C	RMU-Split	0.43	0.55	—	—	—	—	0.40	0.53
B, C	L-RMU-Split	0.35	0.49	—	—	—	—	0.56	0.56
B, D	RMU	0.45	0.56	—	—	0.44	0.46	—	—
B, D	L-RMU	0.35	0.51	—	—	0.42	0.47	—	—
B, D	RMU-Split	0.45	0.55	—	—	0.39	0.46	—	—
B, D	L-RMU-Split	0.34	0.49	—	—	0.39	0.49	—	—
C, D	RMU	0.43	0.54	0.42	0.48	—	—	—	—
C, D	L-RMU	0.27	0.47	0.35	0.45	—	—	—	—
C, D	RMU-Split	0.36	0.55	0.38	0.48	—	—	—	—
C, D	L-RMU-Split	0.29	0.48	0.41	0.51	—	—	—	—
A, B, C	RMU	—	—	—	—	—	—	0.46	0.52
A, B, C	L-RMU	—	—	—	—	—	—	0.49	0.56
A, B, C	RMU-Split	—	—	—	—	—	—	0.42	0.53
A, B, C	L-RMU-Split	—	—	—	—	—	—	0.59	0.56

Continued on next page

Continued from previous page

Relearn	Method	A ↓		B ↓		C ↓		D ↓	
		MCQ	Corpus	MCQ	Corpus	MCQ	Corpus	MCQ	Corpus
A, B, D	RMU	—	—	—	—	0.44	0.48	—	—
A, B, D	L-RMU	—	—	—	—	0.42	0.51	—	—
A, B, D	RMU-Split	—	—	—	—	0.42	0.47	—	—
A, B, D	L-RMU-Split	—	—	—	—	0.45	0.49	—	—
A, C, D	RMU	—	—	0.48	0.49	—	—	—	—
A, C, D	L-RMU	—	—	0.39	0.48	—	—	—	—
A, C, D	RMU-Split	—	—	0.49	0.49	—	—	—	—
A, C, D	L-RMU-Split	—	—	0.43	0.51	—	—	—	—
B, C, D	RMU	0.47	0.55	—	—	—	—	—	—
B, C, D	L-RMU	0.31	0.51	—	—	—	—	—	—
B, C, D	RMU-Split	0.44	0.57	—	—	—	—	—	—
B, C, D	L-RMU-Split	0.37	0.48	—	—	—	—	—	—

522 **E.4 MMLU 3 folds**

Table 11: Relearning accuracy across methods for MMLU 3 folds.

Relearn	Method	A ↓		B ↓		C ↓	
		MCQ	Corpus	MCQ	Corpus	MCQ	Corpus
A	RMU	—	—	0.49	0.66	0.51	0.64
A	L-RMU	—	—	0.40	0.61	0.56	0.64
A	RMU-Split	—	—	0.52	0.63	0.48	0.62
A	L-RMU-Split	—	—	0.40	0.57	0.50	0.64
B	RMU	0.52	0.65	—	—	0.51	0.62
B	L-RMU	0.30	0.54	—	—	0.59	0.64
B	RMU-Split	0.50	0.63	—	—	0.49	0.62
B	L-RMU-Split	0.38	0.61	—	—	0.49	0.63
C	RMU	0.53	0.64	0.52	0.64	—	—
C	L-RMU	0.33	0.39	0.39	0.46	—	—
C	RMU-Split	0.55	0.65	0.57	0.64	—	—
C	L-RMU-Split	0.36	0.48	0.38	0.50	—	—
A, B	RMU	—	—	—	—	0.54	0.63
A, B	L-RMU	—	—	—	—	0.60	0.64
A, B	RMU-Split	—	—	—	—	0.61	0.64
A, B	L-RMU-Split	—	—	—	—	0.53	0.63
A, C	RMU	—	—	0.55	0.64	—	—
A, C	L-RMU	—	—	0.44	0.61	—	—
A, C	RMU-Split	—	—	0.61	0.66	—	—
A, C	L-RMU-Split	—	—	0.48	0.59	—	—
B, C	RMU	0.52	0.65	—	—	—	—
B, C	L-RMU	0.32	0.55	—	—	—	—
B, C	RMU-Split	0.53	0.67	—	—	—	—
B, C	L-RMU-Split	0.38	0.60	—	—	—	—

523 **E.5 Years 3 folds**

Table 12: Relearning accuracy across methods for Years 3 folds.

Relearn	Method	A ↓		B ↓		C ↓	
		MCQ	Corpus	MCQ	Corpus	MCQ	Corpus
A	RMU	—	—	0.55	0.57	0.55	0.58
A	L-RMU	—	—	0.47	0.45	0.50	0.53
A	RMU-Split	—	—	0.55	0.48	0.54	0.48
A	L-RMU-Split	—	—	0.43	0.36	0.51	0.50
B	RMU	0.56	0.59	—	—	0.55	0.58
B	L-RMU	0.40	0.33	—	—	0.51	0.51
B	RMU-Split	0.59	0.48	—	—	0.49	0.52
B	L-RMU-Split	0.37	0.33	—	—	0.52	0.52
C	RMU	0.54	0.58	0.58	0.58	—	—
C	L-RMU	0.29	0.32	0.43	0.42	—	—
C	RMU-Split	0.54	0.46	0.54	0.47	—	—
C	L-RMU-Split	0.29	0.31	0.42	0.38	—	—
A, B	RMU	—	—	—	—	0.61	0.58
A, B	L-RMU	—	—	—	—	0.51	0.52
A, B	RMU-Split	—	—	—	—	0.59	0.54
A, B	L-RMU-Split	—	—	—	—	0.56	0.53
A, C	RMU	—	—	0.61	0.57	—	—
A, C	L-RMU	—	—	0.52	0.45	—	—
A, C	RMU-Split	—	—	0.60	0.51	—	—
A, C	L-RMU-Split	—	—	0.51	0.42	—	—
B, C	RMU	0.62	0.59	—	—	—	—
B, C	L-RMU	0.43	0.32	—	—	—	—
B, C	RMU-Split	0.59	0.50	—	—	—	—
B, C	L-RMU-Split	0.40	0.34	—	—	—	—

F Hyperparameters

We set the forgetting threshold to 0.35, motivated by the following statistical reasoning.

For multiple-choice questions (MCQ) with 4 choices, assuming random guessing, the expected accuracy is 0.25. Each dataset contains a total of 735 questions, and the smallest fold we consider consists of $\frac{735}{4}$. By applying the central limit theorem, the expected final accuracy follows approximately a normal distribution:

$$\mathcal{N}\left(\frac{1}{4}, \sqrt{\frac{1}{4} \cdot \frac{3}{4} \cdot \frac{4}{735}}\right) \approx \mathcal{N}(0.25, 0.032).$$

A three-standard-deviation event corresponds to:

$$3 \times 0.032 + 0.25 \leq 0.35.$$

Since we do not reject the null hypothesis of random guessing if accuracy remains within three standard deviations of 0.25, we set the forgetting threshold to approximately 0.35. Note that this bound does get tighter if we consider bigger folds, but in practice, we find that this threshold does not significantly impact results, so we standardize it across all instances of LU.

For all models, we use Zephyr-7B- β (Tunstall et al., 2023).

F.1 RMU hyperparameters

WMDP: official model checkpoint from (Li et al., 2024a). MMLU:

- Activation layer: 7.
- Layers fine-tuned: 5, 6, 7.
- Magnitude: 10.
- Forget coefficient: 2.00.
- Retain coefficient: 16.00.
- Learning rate: 5×10^{-5} .
- Batch size: 4.

Years:

- Activation layer: 7.
- Layers fine-tuned: 5, 6, 7.
- Magnitude: 15.
- Forget coefficient: 0.25.
- Retain coefficient: 1.00.
- Learning rate: 5×10^{-5} .
- Batch size: 4.

F.2 RMU-Split hyperparameters

WMDP 2 folds:

- Activation layer: 7.
- Layers fine-tuned: 5, 6, 7.
- Magnitude: 10.
- Forget coefficients: 1.00, 1.00.
- Retain coefficient 32.

- 561 • Learning rate: 1×10^{-5} .
- 562 • Batch size: 4.

563 WMDP 3 folds:

- 564 • Activation layer: 7.
- 565 • Layers fine-tuned: 5, 6, 7.
- 566 • Magnitude: 10.
- 567 • Forget coefficients: 1.00, 1.00, 1.00.
- 568 • Retain coefficient 16.
- 569 • Learning rate: 1×10^{-5} .
- 570 • Batch size: 4.

571 WMDP 4 folds:

- 572 • Activation layer: 7.
- 573 • Layers fine-tuned: 5, 6, 7.
- 574 • Magnitude: 10.
- 575 • Forget coefficients: 1.00, 1.00, 1.00, 1.00.
- 576 • Retain coefficient 32.
- 577 • Learning rate: 1×10^{-5} .
- 578 • Batch size: 4.

579 MMLU 3 folds:

- 580 • Activation layer: 7.
- 581 • Layers fine-tuned: 5, 6, 7.
- 582 • Magnitude: 10.
- 583 • Forget coefficients: 2.00, 2.00, 2.00.
- 584 • Retain coefficient 24.
- 585 • MMLU retain coefficient: 12.0.
- 586 • Learning rate: 1×10^{-5} .
- 587 • Batch size: 8.

588 Years 3 folds:

- 589 • Activation layer: 7.
- 590 • Layers fine-tuned: 5, 6, 7.
- 591 • Magnitude: 10.
- 592 • Forget coefficients: 1.00, 1.00, 1.00.
- 593 • Retain coefficient 32.
- 594 • Learning rate: 1×10^{-5} .
- 595 • Batch size: 4.

596 **F.3 L-RMU hyperparameters**

597 WMDP 2 folds:

- 598 • Stage 1:
 - 599 – Activation layer: 7.

- 600 – Layers fine-tuned: 5, 6, 7.
- 601 – Magnitude: 6.5.
- 602 – Forget coefficients: 0.39, 0.00.
- 603 – Retain coefficients: 0.00, 13.52.
- 604 – Retain set coefficient: 1.
- 605 – Learning rate: 1×10^{-5} .
- 606 – Batch size: 4.
- 607 • Stage 2:
 - 608 – Activation layer: 7.
 - 609 – Layers fine-tuned: 5, 6, 7.
 - 610 – Magnitude: 6.5.
 - 611 – Forget coefficients: 0.10, 1.00.
 - 612 – Retain coefficients: 0.00, 0.00.
 - 613 – Retain set coefficient: 24.
 - 614 – Learning rate: 1×10^{-5} .
 - 615 – Batch size: 8.

616 WMDP 3 folds:

- 617 • Stage 1:
 - 618 – Activation layer: 7.
 - 619 – Layers fine-tuned: 5, 6, 7.
 - 620 – Magnitude: 6.5.
 - 621 – Forget coefficients: 0.39, 0.00, 0.00.
 - 622 – Retain coefficients: 0.00, 6.76, 6.76.
 - 623 – Retain set coefficient: 1.
 - 624 – Learning rate: 1×10^{-5} .
 - 625 – Batch size: 4.
- 626 • Stage 2:
 - 627 – Activation layer: 7.
 - 628 – Layers fine-tuned: 5, 6, 7.
 - 629 – Magnitude: 6.5.
 - 630 – Forget coefficients: 0.05, 0.50, 0.00.
 - 631 – Retain coefficients: 0.00, 0.00, 8.00.
 - 632 – Retain set coefficient: 16.
 - 633 – Learning rate: 1×10^{-5} .
 - 634 – Batch size: 8.
- 635 • Stage 3:
 - 636 – Activation layer: 7.
 - 637 – Layers fine-tuned: 5, 6, 7.
 - 638 – Magnitude: 6.5.
 - 639 – Forget coefficients: 0.00, 0.03, 0.33.
 - 640 – Retain coefficients: 0.00, 0.00, 0.00.
 - 641 – Retain set coefficient: 24.
 - 642 – Learning rate: 1×10^{-5} .
 - 643 – Batch size: 8.

644 WMDP 4 folds:

- 645 • Stage 1:
 - 646 – Activation layer: 7.

- 647 – Layers fine-tuned: 5, 6, 7.
- 648 – Magnitude: 6.5.
- 649 – Forget coefficients: 0.39, 0.00, 0.00, 0.00.
- 650 – Retain coefficients: 0.00, 10.67, 10.67, 10.67.
- 651 – Retain set coefficient: 1.
- 652 – Learning rate: 1×10^{-5} .
- 653 – Batch size: 4.
- 654 • Stage 2:
 - 655 – Activation layer: 7.
 - 656 – Layers fine-tuned: 5, 6, 7.
 - 657 – Magnitude: 6.5.
 - 658 – Forget coefficients: 0.10, 1.00, 0.00, 0.00.
 - 659 – Retain coefficients: 0.00, 0.00, 4.00, 4.00.
 - 660 – Retain set coefficient: 16.
 - 661 – Learning rate: 1×10^{-5} .
 - 662 – Batch size: 8.
- 663 • Stage 3:
 - 664 – Activation layer: 7.
 - 665 – Layers fine-tuned: 5, 6, 7.
 - 666 – Magnitude: 6.5.
 - 667 – Forget coefficients: 0.01, 0.07, 0.67, 0.00.
 - 668 – Retain coefficients: 0.00, 0.00, 0.00, 8.00.
 - 669 – Retain set coefficient: 16.
 - 670 – Learning rate: 1×10^{-5} .
 - 671 – Batch size: 8.
- 672 • Stage 4:
 - 673 – Activation layer: 7.
 - 674 – Layers fine-tuned: 5, 6, 7.
 - 675 – Magnitude: 6.5.
 - 676 – Forget coefficients: 0.01, 0.03, 0.15, 0.75.
 - 677 – Retain coefficients: 0.00, 0.00, 0.00, 0.00.
 - 678 – Retain set coefficient: 32.
 - 679 – Learning rate: 1×10^{-5} .
 - 680 – Batch size: 8.

681 MMLU 3 folds:

- 682 • Stage 1:
 - 683 – Activation layer: 7.
 - 684 – Layers fine-tuned: 5, 6, 7.
 - 685 – Magnitude: 6.5.
 - 686 – Forget coefficients: 2.00, 0.00, 0.00.
 - 687 – Retain coefficients: 0.00, 8.00, 8.00.
 - 688 – Retain set coefficient: 2.
 - 689 – Learning rate: 1×10^{-5} .
 - 690 – Batch size: 4.
- 691 • Stage 2:
 - 692 – Activation layer: 7.
 - 693 – Layers fine-tuned: 5, 6, 7.
 - 694 – Magnitude: 6.5.

- 695 – Forget coefficients: 0.10, 2.00, 0.00.
- 696 – Retain coefficients: 0.00, 0.00, 4.00.
- 697 – Retain set coefficient: 32.
- 698 – MMLU retain coefficient: 8.0.
- 699 – Learning rate: 1×10^{-5} .
- 700 – Batch size: 8.
- 701 • Stage 3:
 - 702 – Activation layer: 7.
 - 703 – Layers fine-tuned: 5, 6, 7.
 - 704 – Magnitude: 6.5.
 - 705 – Forget coefficients: 0.01, 0.13, 2.67.
 - 706 – Retain coefficients: 0.00, 0.00, 0.00.
 - 707 – Retain set coefficient: 36.
 - 708 – MMLU retain coefficient: 18.0.
 - 709 – Learning rate: 1×10^{-5} .
 - 710 – Batch size: 8.

711 Years 3 folds:

- 712 • Stage 1:
 - 713 – Activation layer: 7.
 - 714 – Layers fine-tuned: 5, 6, 7.
 - 715 – Magnitude: 6.5.
 - 716 – Forget coefficients: 4.00, 0.00, 0.00.
 - 717 – Retain coefficients: 0.00, 16.00, 16.00.
 - 718 – Retain set coefficient: 2.
 - 719 – Learning rate: 1×10^{-5} .
 - 720 – Batch size: 4.
- 721 • Stage 2:
 - 722 – Activation layer: 7.
 - 723 – Layers fine-tuned: 5, 6, 7.
 - 724 – Magnitude: 6.5.
 - 725 – Forget coefficients: 2.25, 22.50, 0.00.
 - 726 – Retain coefficients: 0.00, 0.00, 16.00.
 - 727 – Retain set coefficient: 16.
 - 728 – Learning rate: 1×10^{-5} .
 - 729 – Batch size: 8.
- 730 • Stage 3:
 - 731 – Activation layer: 7.
 - 732 – Layers fine-tuned: 5, 6, 7.
 - 733 – Magnitude: 6.5.
 - 734 – Forget coefficients: 0.15, 1.50, 15.00.
 - 735 – Retain coefficients: 0.00, 0.00, 0.00.
 - 736 – Retain set coefficient: 32.
 - 737 – Learning rate: 1×10^{-5} .
 - 738 – Batch size: 8.

F.4 L-RMU-Split hyperparameters

WMDP 2 folds:

- Stage 1:
 - Activation layer: 7.
 - Layers fine-tuned: 5, 6, 7.
 - Magnitude: 6.5.
 - Forget coefficients: 0.39, 0.00.
 - Retain coefficients: 0.00, 13.52.
 - Retain set coefficient: 1.
 - Learning rate: 1×10^{-5} .
 - Batch size: 4.
- Stage 2:
 - Activation layer: 7.
 - Layers fine-tuned: 5, 6, 7.
 - Magnitude: 6.5.
 - Forget coefficients: 0.10, 0.20.
 - Retain coefficients: 0.00, 0.00.
 - Retain set coefficient: 14.51609.
 - Learning rate: 1×10^{-5} .
 - Batch size: 4.

WMDP 3 folds:

- Stage 1:
 - Activation layer: 7.
 - Layers fine-tuned: 5, 6, 7.
 - Magnitude: 6.5.
 - Forget coefficients: 0.39, 0.00, 0.00.
 - Retain coefficients: 0.00, 6.76, 6.76.
 - Retain set coefficient: 1.
 - Learning rate: 1×10^{-5} .
 - Batch size: 4.
- Stage 2:
 - Activation layer: 7.
 - Layers fine-tuned: 5, 6, 7.
 - Magnitude: 6.5.
 - Forget coefficients: 1.00, 4.00, 0.00.
 - Retain coefficients: 0.00, 0.00, 13.52.
 - Retain set coefficient: 32.
 - Learning rate: 3×10^{-6} .
 - Batch size: 4.
- Stage 3:
 - Activation layer: 7.
 - Layers fine-tuned: 5, 6, 7.
 - Magnitude: 6.5.
 - Forget coefficients: 0.33, 1.33, 5.33.
 - Retain coefficients: 0.00, 0.00, 0.00.
 - Retain set coefficient: 45.51609.
 - Learning rate: 3×10^{-6} .

786 – Batch size: 12.

787 WMDP 4 folds:

- 788 • Stage 1:
 - 789 – Activation layer: 7.
 - 790 – Layers fine-tuned: 5, 6, 7.
 - 791 – Magnitude: 6.5.
 - 792 – Forget coefficients: 0.39, 0.00, 0.00, 0.00.
 - 793 – Retain coefficients: 0.00, 10.67, 10.67, 10.67.
 - 794 – Retain set coefficient: 1.
 - 795 – Learning rate: 1×10^{-5} .
 - 796 – Batch size: 4.
- 797 • Stage 2:
 - 798 – Activation layer: 7.
 - 799 – Layers fine-tuned: 5, 6, 7.
 - 800 – Magnitude: 6.5.
 - 801 – Forget coefficients: 0.10, 0.20, 0.00, 0.00.
 - 802 – Retain coefficients: 0.00, 0.00, 16.00, 16.00.
 - 803 – Retain set coefficient: 8.
 - 804 – Learning rate: 1×10^{-5} .
 - 805 – Batch size: 4.
- 806 • Stage 3:
 - 807 – Activation layer: 7.
 - 808 – Layers fine-tuned: 5, 6, 7.
 - 809 – Magnitude: 6.5.
 - 810 – Forget coefficients: 0.03, 0.07, 0.13, 0.00.
 - 811 – Retain coefficients: 0.00, 0.00, 0.00, 32.00.
 - 812 – Retain set coefficient: 16.
 - 813 – Learning rate: 1×10^{-5} .
 - 814 – Batch size: 4.
- 815 • Stage 4:
 - 816 – Activation layer: 7.
 - 817 – Layers fine-tuned: 5, 6, 7.
 - 818 – Magnitude: 6.5.
 - 819 – Forget coefficients: 0.03, 0.06, 0.12, 0.25.
 - 820 – Retain coefficients: 0.00, 0.00, 0.00, 0.00.
 - 821 – Retain set coefficient: 32.
 - 822 – Learning rate: 1×10^{-5} .
 - 823 – Batch size: 4.

824 MMLU 3 folds:

- 825 • Stage 1:
 - 826 – Activation layer: 7.
 - 827 – Layers fine-tuned: 5, 6, 7.
 - 828 – Magnitude: 6.5.
 - 829 – Forget coefficients: 2.00, 0.00, 0.00.
 - 830 – Retain coefficients: 0.00, 8.00, 8.00.
 - 831 – Retain set coefficient: 2.
 - 832 – Learning rate: 1×10^{-5} .

- 833 – Batch size: 4.
- 834 • Stage 2:
 - 835 – Activation layer: 7.
 - 836 – Layers fine-tuned: 5,6,7.
 - 837 – Magnitude: 6.5.
 - 838 – Forget coefficients: 0.10,2.00,0.00.
 - 839 – Retain coefficients: 0.00,0.00,8.00.
 - 840 – Retain set coefficient: 32.
 - 841 – MMLU retain coefficient: 8.0.
 - 842 – Learning rate: 1×10^{-5} .
 - 843 – Batch size: 4.
- 844 • Stage 3:
 - 845 – Activation layer: 7.
 - 846 – Layers fine-tuned: 5,6,7.
 - 847 – Magnitude: 10.
 - 848 – Forget coefficients: 0.00,0.07,1.33.
 - 849 – Retain coefficients: 0.00,0.00,0.00.
 - 850 – Retain set coefficient: 40.
 - 851 – MMLU retain coefficient: 10.0.
 - 852 – Learning rate: 1×10^{-5} .
 - 853 – Batch size: 4.
- 854 Years 3 folds:
 - 855 • Stage 1:
 - 856 – Activation layer: 7.
 - 857 – Layers fine-tuned: 5,6,7.
 - 858 – Magnitude: 6.5.
 - 859 – Forget coefficients: 4.00,0.00,0.00.
 - 860 – Retain coefficients: 0.00,16.00,16.00.
 - 861 – Retain set coefficient: 2.
 - 862 – Learning rate: 1×10^{-5} .
 - 863 – Batch size: 4.
 - 864 • Stage 2:
 - 865 – Activation layer: 7.
 - 866 – Layers fine-tuned: 5,6,7.
 - 867 – Magnitude: 12.
 - 868 – Forget coefficients: 1.20,4.00,0.00.
 - 869 – Retain coefficients: 0.00,0.00,32.00.
 - 870 – Retain set coefficient: 2.
 - 871 – Learning rate: 1×10^{-5} .
 - 872 – Batch size: 4.
 - 873 • Stage 3:
 - 874 – Activation layer: 7.
 - 875 – Layers fine-tuned: 5,6,7.
 - 876 – Magnitude: 12.
 - 877 – Forget coefficients: 0.17,0.67,2.67.
 - 878 – Retain coefficients: 0.00,0.00,0.00.
 - 879 – Retain set coefficient: 36.
 - 880 – Learning rate: 1×10^{-5} .
 - 881 – Batch size: 4.

E.5 SimNPO hyperparameters

WMDP:

- Beta: 0.1.
- Forget coefficients: 8.00.
- Retain coefficients: 1.00.
- Learning rate: 4×10^{-6} .
- Batch size: 4.

We reran SimNPO with our own implementation as the checkpoint online did not sufficiently unlearn the data on our folds.

E.6 L-SimNPO hyperparameters

WMDP 3 folds:

- Stage 1:
 - Beta: 0.1.
 - Forget coefficients: 3.00, 0.00, 0.00.
 - Retain coefficients: 0.00, 1.00, 1.00.
 - Retain set coefficient: 4.
 - Learning rate: 4×10^{-6} .
 - Batch size: 4.
- Stage 2:
 - Beta: 0.1.
 - Forget coefficients: 0.60, 3.00, 0.00.
 - Retain coefficients: 0.00, 0.00, 1.00.
 - Retain set coefficient: 6.
 - Learning rate: 4×10^{-6} .
 - Batch size: 4.
- Stage 3:
 - Beta: 0.1.
 - Forget coefficients: 5.00, 5.00, 5.00.
 - Retain coefficients: 0.00, 0.00, 0.00.
 - Retain set coefficient: 6.
 - Learning rate: 4×10^{-6} .
 - Batch size: 4.